DYNAMIC MODELING AND ANALYSIS OF SPINNING POLYGON ASSEMBLIES USING MSC/NASTRAN

Bill Nowak Courtney James

Corporate Research & Technology
Xerox Corporation
800 Phillips Road
Webster, NY 14580

ABSTRACT

This paper describes the application of the MSC/NASTRAN to calculate the dynamic response of a spinning polygon, motor, and motor housing used in xerographic printers. Initially, different levels of model sophistication were evaluated showing convergence to a representative model. Using the converged model, the dynamic response of the polygon mirror was evaluated from the effects of base excitation. Frequency correlation in the 0 to 1000 hertz range was demonstrated to be better than 10% when compared to a dynamic modal test. Mechanical gain correlation at the fundamental rotor resonance was of the same order as the modal test with amplitude variations attributed to the assumed damping of the model, and differences between empirical and analytical response locations. Conclusions and recommendations on future work are also cited.

1. INTRODUCTION

As with any complicated optical system, the dynamic behavior of the mechanical structure which locates, holds and/or moves the optical components is critical to the performance of that system. In the case of a xerographic laser printer, the motor/polygon assembly (MPA), is one of many critical optical components which can be effected by external vibration. The analysis of vibration effects on MPA's is one of several areas where the motion effects on laser beam spot placement need be well understood so these products will produce high quality xerographic prints for a very demanding and competitive marketplace.

A cursory search of the literature indicated that very little work related to vibration of laser printheads has been published. Structural dynamic effects on overall printhead vibration has been addressed previously[1] but in that case the MPA was assumed to be a rigid assembly only affected by the flexibility of the surrounding structure. Internal empirical vibration assessment of the same MPA used in this paper was completed[2] citing two main frequencies of vibration in the 0 to 1000 hertz range and a dependency on axial preload of the bearing. Frequency response data was not presented and was later completed for comparison with the analysis conducted herein.

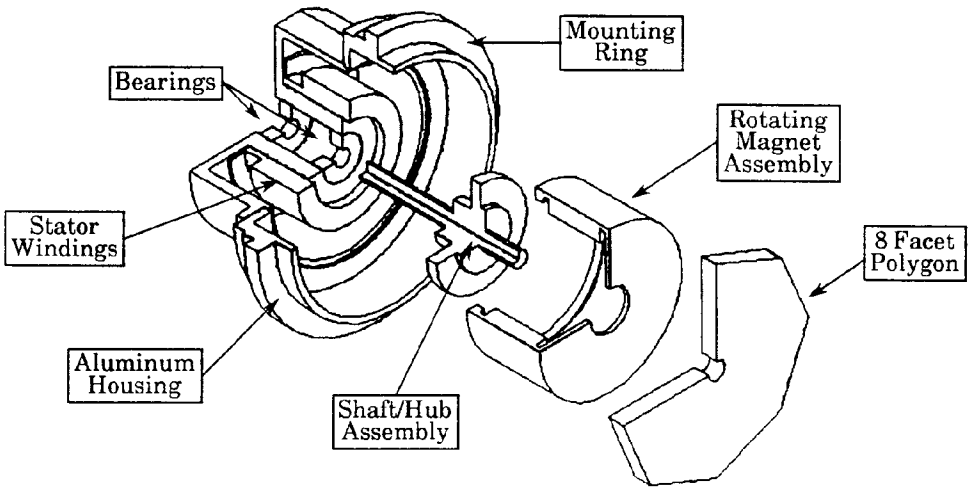

Figure 1. Schematic of motor / polygon assembly showing basic components.

A schematic of the MPA analyzed is shown in figure 1. The key components of the assembly are as follows: an aluminum outer housing assembly; a pair of ball bearing shaft supports; a stator winding coil; a stainless steel shaft with an aluminum press-fit hub; a rotating magnet assembly consisting of a steel cup and four permanent ceramic magnets bonded to the inside surface; and an 8 facet aluminum polygon. The polygon and rotating magnet assembly are secured to the hub of the shaft. This shaft assembly is then supported in the outer housing by the two ball bearings. The entire assembly is mounted within the laser print head via three mounting points around the perimeter ring of the outer housing.

This is one of many optical components in a laser print head, commonly referred to as a raster output scanner (ROS). A typical ROS is composed of numerous output beam conditioning lenses and turning mirrors used to fold the required optical path length into a structure of manageable size as shown in Figure 2. A beam is emitted from a helium-neon laser, through a series of pre-polygon conditioning lenses and turning mirrors, onto the rotating polygon mirror. The high speed rotation of the polygon, which is usually in the 3 to 15 krpm range, then scans the beam through a series of post-polygon conditioning lenses and onto a final turning mirror, and images the laser spot across the full process width at the image plane as the photoconductor surface passes by. An electronic subsystem, which

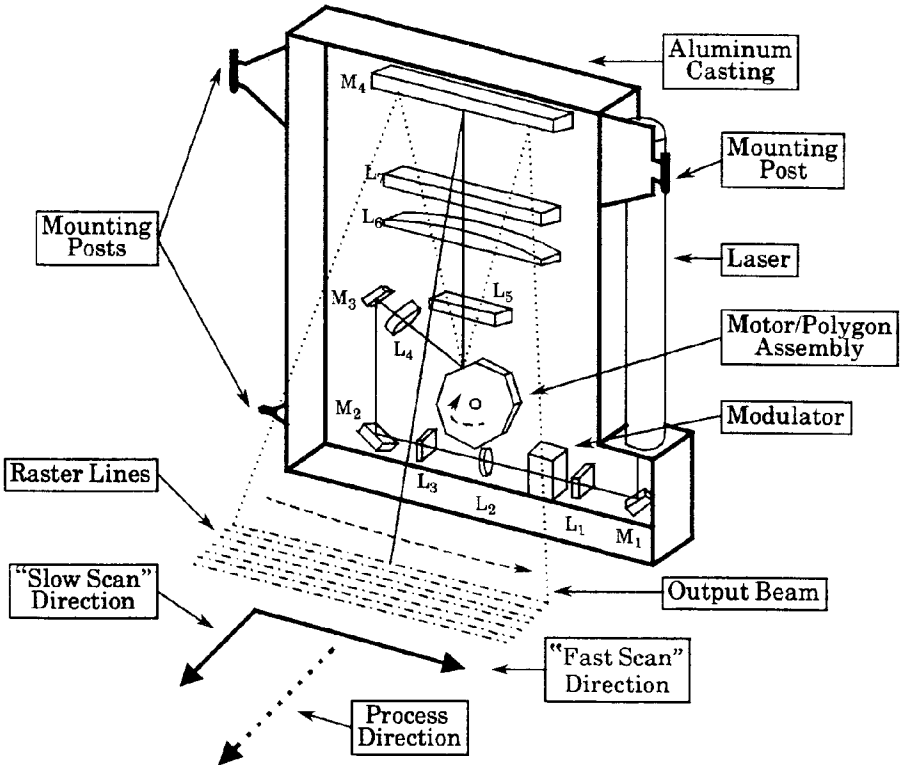

Figure 2. Schematic of a raster output scanner (ROS) .

processes the digital information, directs the modulator to deflect the laser beam "on to" or "off of" a light stop which turns the laser spot on or off at the photoconductor surface. The laser beam discharges areas on the photoconductor where dry ink is not intended to adhere, leaving areas charged where dry ink is intended to adhere

2. MOTOR / POLYGON ASSEMBLY MODEL DEVELOPMENT

The finite element method[3], FEMAP[4] and MSC/NASTRAN[5] were used to model and analyze the MPA. Models 1 through 4 in figure 3 are representations of the rotor assembly of the MPA. These models depict varying degrees of complexity, with Model 1 being the least refined and Model 4 being the most. Model 5 represents the complete MPA, consisting of the most refined rotor assembly model (Model 4) combined with a model of the outer housing assembly.

In Model 1, the stainless steel shaft is modeled with 20 BEAM elements and 21 GRID points with other main MPA components appropriately lumped. The polygon and rotating magnet assembly are each represented by CONM2 elements and the aluminum pressed hub is represented by 3 short BEAMS having cross-sectional properties consistent with that of the hub's three sections. This shaft assembly is supported by 2 rigid "knife-edge" bearings tied to ground using SPC's such that translations at the shaft mounting points are constrained.

Model 2 is similar to Model 1, but with the aluminum pressed hub and polygon no longer being lumped. The polygon and pressed hub are modeled by 64 and 126 HEXA and PENTA elements, respectively. The polygon is fixed to the hub, and the hub and polygon are attached to the shaft with RBE2 elements. In both cases the radial degree of freedom was left free to allow for radial expansion of the hub and polygon due to centrifugal loading. The number of GRID points in Model 2 totals 451.

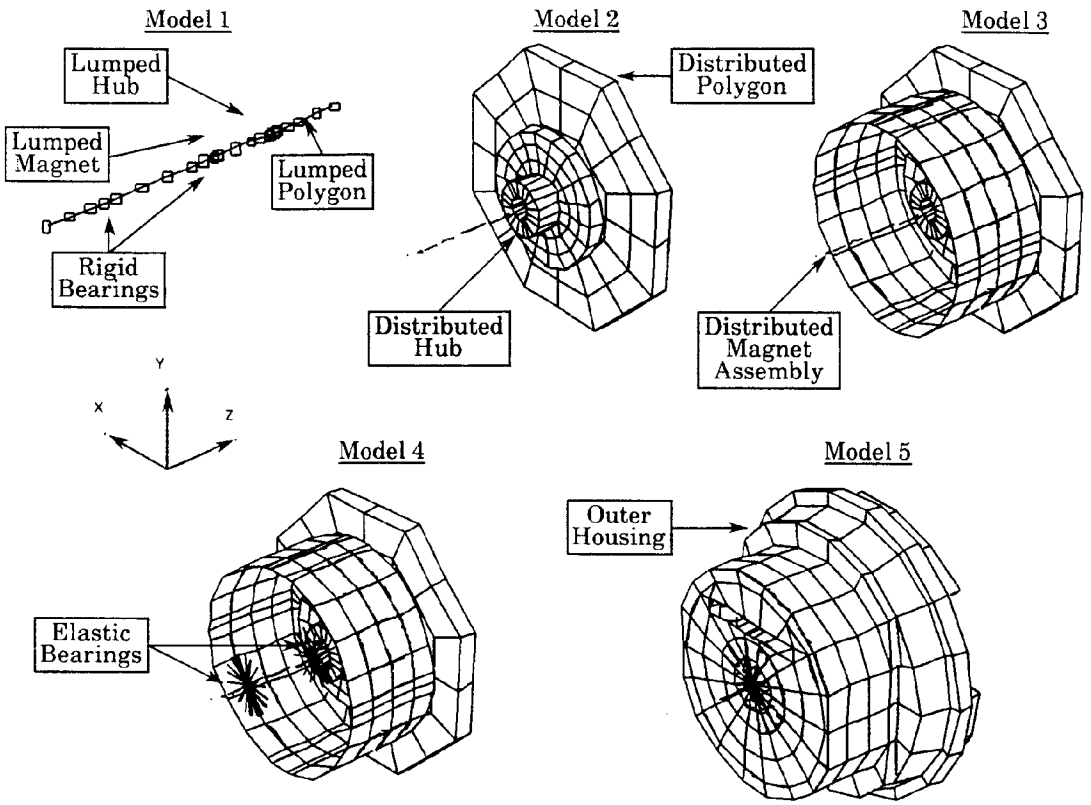

Figure 3. Motor / polygon assembly finite element model development.

Model 3 differs from Model 2 in that the rotating magnet assembly is no longer lumped. The steel cup of the assembly is modeled by 166 QUAD4 and TRIA3 elements and attached to the hub at 3 mounting points via rigid elements. The ceramic magnets are modeled with 60 QUAD4 and TRIA3 elements and share coincident nodes with the area of the cup that they cover. To properly represent the location of each magnet with respect to the section of the cup that it was attached to, "z-offsets" were used to move each magnet's midplane off of the midplane of the corresponding cup area. As a result of the additional model definition, the number of GRID points in model 3 increased to 635.

Model 4 is similar to Model 3, except for a change in shaft assembly mounting conditions. The bearings are modeled with a representative radial stiffness instead of the rigid condition previously assumed. For each bearing, this is accomplished by a set of 18 ROD elements arranged cirumferentially about the shaft mounting location. This model now totals 678 GRID points.

Model 5 represents the complete MPA and consists of the rotor assembly and elastic bearings of Model 4 mounted to a model of the outer housing assembly of the MPA. The outer housing consists of 112 QUAD4 and TRIA3 elements and 246 HEXA and PENTA elements. The MPA model is attached at the three mounting points on the housing to a input node via an RBE2 element. This single input GRID can be fixed or used to input excitations for frequency response calculations. Because of the additional structure modeled, the total number of GRID points is increased to 1230.

3. NATURAL FREQUENCY AND MODESHAPE COMPARISON

At the beginning of this modeling effort, it was not clear what degree of sophistication was necessary to get a representative model of the MPA in the frequency range desired. Reviewing the results in table 1 clearly shows that not only a great deal of modeling sophistication of the spinning rotor is necessary, but also the detailed representation of the aluminum housing which mounts the shaft bearings is necessary for good frequency correlation. When compared to a modal test conducted by Costanza[2], only Model 5 produced better than 10% frequency correlation for the 1st and 2nd modes of vibration.

Table 1. MPA bending modes of vibration in 0 to 1000 hertz range.

Frequency Number	Model 1	Model 2	Model 3	Model 4	Model 5	Empirical	Modeshape Description
f_0	0.0	0.0	0.0	0.0	0.0	0.0	Rigid Body
f_1	609 hz	547 hz	510hz	463 hz	395 hz	425 hz	1st Bending Y-Z Plane
f_2	609 hz	561 hz	512 hz	464 hz	419 hz	-	1st Bending X-Z Plane
f_3	-	-	-	-	665 hz	650 hz	2nd Bending Y-Z Plane
f_4	-	-	-	-	691 hz	-	2nd Bending X-Z Plane

Figure 4 show the 1st and 2nd bending modes of vibration for frequencies f_1 and f_4, respectively. The modeshapes for frequencies f_2 and f_3 are not shown but vibrate in planes orthogonal to the ones depicted below.

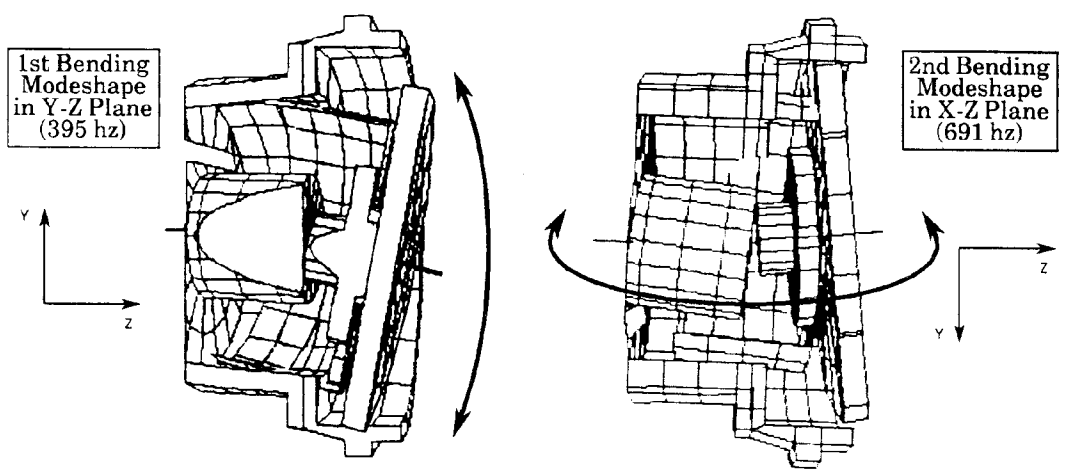

Figure 4. 1st bending mode in Y-Z plane and 2nd bending mode in X-Z plane of MPA Model 5.

4. FREQUENCY RESPONSE DUE TO BASE EXCITATION

Once reasonable frequency correlation was achieved with Model 5, a dynamic response calculation was made over the frequency range of 0 to 1000 hz. In situ, the MPA would be mounted in the ROS housing which intern mounts to the machine frame containing all of the excitation frequencies of the xerographic processor. Since a ROS housing model was not available, it was assumed that the MPA was mounted on a rigid base at 3 screw locations on the mounting ring as previously described. A large mass was placed at the forth point in the rigid mounting structure and a unit force scaled by the same magnitude as the large mass was applied to simulate an enforced base excitation. Unit white noise was applied over the frequency range and a damping value for the MPA was assumed to be of 1% of critical.

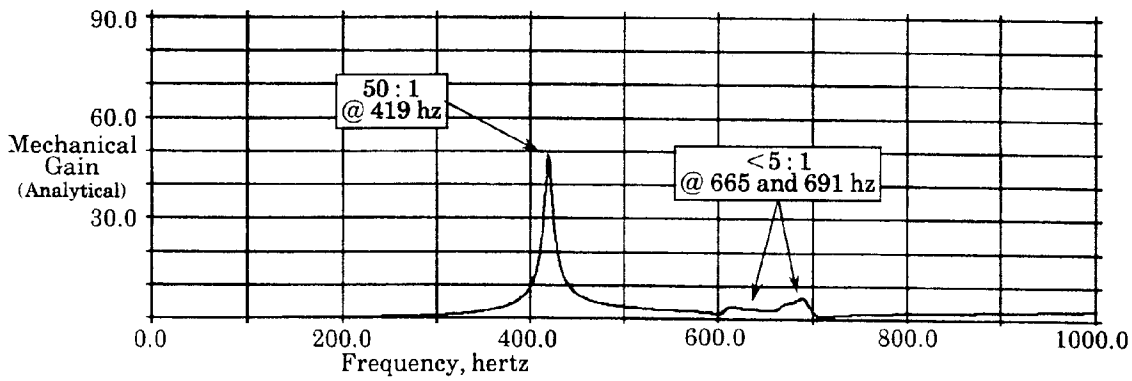

Figure 5. Frequency response of model 5 polygon at center facet in the Z direction due to an X direction base excitation of motor/polygon assembly.

Figure 5 shows the mechanical gain of the polygon facet in the X direction which is parallel to the axis of rotation. Dynamic displacement of the facet in this direction directly relates to raster line misplacement in the "slow scan" direction thus creating xerographic print defects as described in reference 1. Figure 6 shows the corresponding frequency response test conducted on the actual MPA. The MPA was mounted to a rigid frame at the same 3 mounting locations as the model. The frame was then mounted to a shaker table and instrumented with accelerometers to measure input excitation and output response of the MPA at the same positions and directions as were calculated in the analysis. The test and analysis were both conducted at 0 rpm.

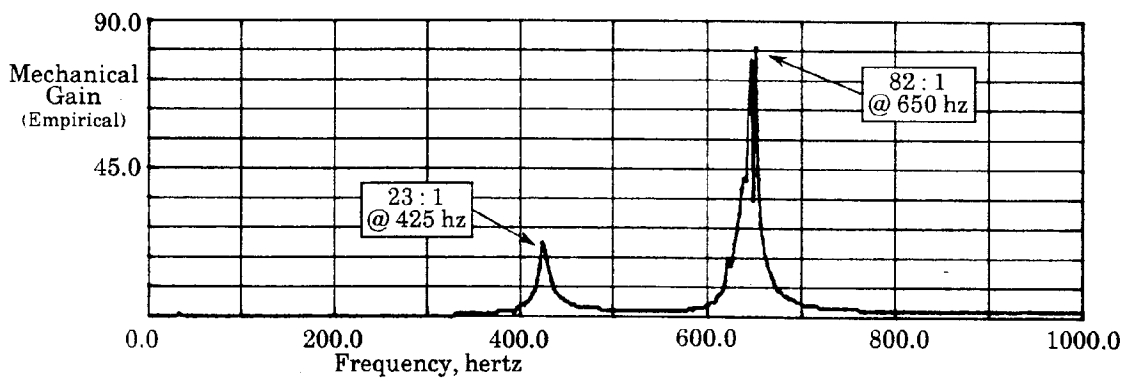

Figure 6. Frequency response of actual polygon at center facet in the Z direction due to an X direction excitation of the motor/polygon assembly on a shaker table.

As noted in figures 5 and 6, the resonant frequencies of the mathematical and empirical systems show good correlation. Differences in response amplitude at the fundamental frequency are attributed to the assumed damping of Model 5 being less than the actual MPA and the accelerometer mounted to the polygon which measured data approximately 0.25 inch below the facet surface. Both of these effects would improve amplitude correlation at the fundamental resonance. Unfortunately, the poor amplitude correlation at the 2nd bending modes of vibration are difficult to understand. The only explanation is that the interactions between the rotating magnet and shaft/hub assemblies, and the polygon were not adequately addressed as necessary for Model 5 to be predictive of these response amplitudes. This hypothesis is partially supported by modeshape deformations between these assemblies in the 2nd bending mode depicted in figure 4.

5. CONCLUSIONS

The modeling and analysis of an MPA were successfully demonstrated in this paper. While amplitude correlation was poor at the higher system resonances, the analysis showed that the finite element method with the correct degree of model sophistication is predictive of the complicated dynamic behavior of the MPA's used in polygon ROS's. It is apparent from this modeling activity that classical text book theory and traditional lumped parameter dynamic models of motor/polygon assemblies would fall far short of predicting dynamic behavior. Thus, the rigor of the finite element method is necessary to predict the dynamic response of these systems.

6. RECOMMENDATIONS

There is a great need for future analysis and test efforts to continue in this technological area. The effects of rotor imbalance and centrifugal stiffening at MPA operating speeds needs to be addressed. Analytical procedures need to be demonstrated and test methods to measure operating system response need to be developed. Future work should also include realistic representation of the ROS and xerographic processor frame as well as the structure which houses the moving photoconductor. All of these factors play into our ability to model, predict, test and build xerographic printers for todays competitive office product marketplace.

7. ACKNOWLEDGMENTS

The authors would like to thank Dan Costanza for assessing the MPA dynamic response on the shaker table and generating the mechanical gain curves used for analytical/empirical comparison.

8. REFERENCES

1. Nowak, W.J., "Structural Dynamic Analysis of Laser Spot Motion in Xerographic Printers," Proceedings of the SPIE's 33rd Annual International Technical Symposium on Optical & Optoelectronic Applied Science and Engineering, August 10, 1989.
2. Costanza, D.W., "Experimental Determination of the Rotor Dynamics of a Motor Polygon Assembly," Xerox internal report, December 1989.
3. Cook, R.D., Concepts and Applications of Finite Element Analysis, 2nd edition,John Wiley & Sons, New York, Copyright 1981.
4. "FEMAP User's Manual, Version 3.0", Enterprise Software Products, Inc., 1989.
5. MSC/NASTRAN User's Manual, Version 65, Vol.I and II, The MacNeal-Schwendler Corp., Los Angeles, California, Copyright 1985.